A new species of marsupial frog (Anura; *Gastrotheca*) from the Cordillera de Colán in northeastern Peru

Pablo J. Venegas[1,2], Luis A. García-Ayachi[1,2], Lourdes Y. Echevarría[2,3], Daniel J. Paluh[4], Juan C. Chávez-Arribasplata[1,2], Axel Marchelie[2], Alessandro Catenazzi[1,2,5]

1 *Instituto Peruano de Herpetología (IPH), Lima, Perú*

2 *División de Herpetología, Centro de Ornitología y Biodiversidad (CORBIDI), Lima, Perú*

3 *Pontifícia Universidade Católica do Rio Grande do Sul (PUCRS), Laboratório de Sistemática de Vertebrados, Porto Alegre, Brazil*

4 *Department of Natural History, Florida Museum of Natural History, University of Florida, Gainesville, Florida, USA*

5 *Department of Biological Sciences, Florida International University, Miami, Florida, USA*

http://zoobank.org/66E0CD18-A7E1-42F1-A8EF-052DE7F60790

Corresponding author: Pablo J. Venegas (pvenegas@corbidi.org)

Citation: Venegas PJ, García-Ayachi LA, Echevarría LY, Paluh DJ, Chávez-Arribasplata JC, Marchelie A, Catenazzi A (2021) A new species of marsupial frog (Anura; *Gastrotheca*) from the Cordillera de Colán in northeastern Peru. Vertebrate Zoology 71: 201–218. https://doi.org/10.3897/vz.71.e60097

Abstract

We describe a new species of marsupial frog, genus *Gastrotheca*, using morphological characters and molecular data as lines of evidence. The new species was discovered in the páramo and the ecotone between páramo and humid montane forest of Cordillera de Colán, at elevations between 3136 and 3179 m a.s.l., in northeastern Peru. The new species is distinguished from all its congeners by the combination of the following characters: coarsely granular skin on dorsum, a green dorsal coloration without pattern, finger I shorter than finger II, turquoise iris, and a venter without blotches, flecks or dots. Furthermore, we include a detailed osteological description of the new *Gastrotheca* species based on Micro-CT scanning. Based on our phylogenetic analyses, the new species belongs to the *Gastrotheca marsupiata* species group, is sister to *G. oresbios* and closely related to *G. psychrophila*, *G. spectabilis*, *G. stictopleura* and one undescribed species. Additionally, we test for the presence of the fungal pathogen *Batrachochytrium dendrobatidis* (*Bd*). No *Bd* infection was detected for *G. gemma* sp. nov. specimens but *Bd* prevalence was detected among syntopic frogs.

Keywords

Introduction

With 75 described species, the genus *Gastrotheca*—commonly known as marsupial frogs because females brood eggs in closed dorsal pouches (Duellman 2015)—is the most speciose genus of the family Hemiphractidae (Frost 2020). Marsupial frogs are particularly diverse along the Andes, from Venezuela to central Argentina, with some species distributed above 4000 m a.s.l. (Duellman 2015). Yet, a number of species are also found in the upper Am-

azon Basin, Cordillera de la Costa and the Atlantic Coastal Forest, as well as in Central America (Blackburn and Duellman 2013; Castroviejo-Fisher et al. 2015; Duellman 2015). In addition to the variety of habitats that marsupial frogs occupy throughout its wide distribution, *Gastrotheca* includes species that undergo direct development, as well as species with an aquatic larval phase (Duellman 2015).

Among the thirty species of *Gastrotheca* that occur in Peru (Frost 2020), 40% have a distribution restricted to the northern Peruvian Andes (Duellman and Venegas 2005, 2016; Duellman 2015). In the Andes of northern Peru, marsupial frogs occur at elevations greater than 1500 m a.s.l. in the northern portion of Cordillera Occidental and Central and in smaller mountain ranges such as Cordillera de Colán, Cordillera del Cóndor, and Cordillera de Huancabamba (Duellman 2015; Duellman and Venegas 2016). However, the herpetofauna of this region is far from being well surveyed and new species of anurans are continuously discovered, especially in remote localities (e.g. Duellman and Venegas 2005; Venegas and Barrio 2005; Lehr and Catenazzi 2011; Rivera-Correa et al. 2016; Rodriguez and Catenazzi 2017).

The Cordillera de Colán is a mountain ridge of moderate elevation in the Andes (< 3700 m a.s.l.), isolated from the main chain of the Andes by the Chiriaco and Utcubamba rivers that flow northward into the upper Marañón River, the main tributary of the Amazon River (Duellman and Pramuk 1999). Few herpetologists have explored these mountains, and most of the herpetological knowledge comes from specimens collected by ornithologists of Louisiana State University (LSU) in 1978. Herpetologists from the University of Kansas described several species of frogs from these LSU specimens, such as *Gastrotheca abdita* Duellman, 1987, *Colostethus spilotogaster* Duellman, 2004, *Eleutherodactylus avicuporum* Duellman & Pramuk, 1999, *E. atrabracus* Duellman & Pramuk, 1999, *E. serendipitus* Duellman & Pramuk, 1999, *E. cuneirostris* Duellman & Pramuk, 1999, *E. metabates* Duellman & Pramuk, 1999, and *Telmatobius colanensis* Wiens, 1993. However, as the herpetofauna from the Cordillera de Colán is still far from being well surveyed, the true dimension of its amphibian biodiversity remains unknown.

The amphibian disease chytridiomycosis has decimated frog communities in Andean montane forests and grasslands (Catenazzi et al. 2011, 2014). Marsupial frogs vary in their vulnerability to chytridiomycosis (Catenazzi et al. 2017), and populations of several species have experienced declines (Scheele et al. 2019). A comparison of skin defences in two sympatric *Gastrotheca* (*Bd*-tolerant *G. excubitor* and *Bd*-susceptible *G. nebulanastes*) supported the hypothesis that anti-*Bd* symbiotic bacteria, rather than skin peptides, may be associated with disease tolerance in marsupial frogs (Burkart et al. 2017). Direct development, associated with a predominantly terrestrial lifestyle, might also limit adult exposure to infective *Bd* zoospores, and eliminates the possibility of larval infection. Nevertheless, considering the catastrophic consequences of *Bd* epizootics in high-Andean frog commu-

nities, it is possible that *Bd* is a major threat to marsupial frogs in northern Peru.

The first author (PJV) conducted two herpetological surveys to the Cordillera de Colán in 2019, and discovered several putative new species of amphibians and reptiles inhabiting the montane forest and páramos of these remote mountains. Herein, we describe a new species of marsupial frog collected in a narrow páramo at the top of this poorly known mountain ridge. We integrate several lines of evidence, including a detailed osteological examination using computed tomography, external meristic and morphological traits, and molecular data to characterize and diagnose the new species. Finally, in recognition of the threat of chytridiomycosis for montane forest and páramo amphibians in the Andes, we quantified pathogen prevalence and intensity of infection in the new species and syntopic frogs.

Materials and methods

Field surveys and skin swabbing for chytrid pathogen detection

We surveyed frogs along existing trails and new open trails during five days, and captured frogs by hand. For each capture, we recorded coordinates and elevation with a GPS (Garmin, WGS84), and we swabbed the skin for detection of the fungal pathogen *Batrachochytrium dendrobatidis*. This procedure does not harm the frogs (Hyatt et al. 2007). Briefly, we gently stroked a sterile rayon-tipped swab (Medical Wire and Equipment MW113) across the skin a total of 30 times per frog: five strokes on each side of the abdominal midline, five strokes on the inner thighs of each hind leg, and five strokes on the foot webbing of each hind leg. We swabbed three specimens of the new species, and 59 specimens of eight species of syntopic frogs. We euthanized voucher specimens with 20% benzocaine gel, fixed them in 10% formalin for 24 hours, and stored them permanently in 70% ethanol. We deposited voucher specimens at the herpetological collection of the Centro de Ornitología y Biodiversidad (CORBIDI) in Lima, Peru.

Morphology

External morphological characters and format of description follow Trueb and Duellman (1978); Duellman and Hillis (1987); Duellman (2015). Coloration features included in the diagnosis refer to coloration in life. We determined sex and maturity of specimens by observing the presence of brood pouches, vocal sac, and vocal slits. We used digital callipers to measure the following meristic traits to the nearest 0.1 mm: snout-vent length (SVL); tibia length: straight-line distance measured between the upper edge of knee and the heel (TIBL); foot length: distance from the proximal edge of the inner metatarsal tubercle to the tip

of the fourth toe (FL); head length: straight-line distance from the posterior edge of the jaw articulation to the tip of the snout (HL); head width: the greatest width of head, measured in a straight line between the posterior edges of the jaw (HW), interorbital distance: straight-line distance between the inner edges of the upper eyelid (IOD); eyelid-width: the greatest width of the upper eyelid, measured from its medial most edge to its outer margin (EW); internarial distance: the distance between the openings of the nostrils (IND); eye diameter: the greatest length of the orbit (ED); eye-nostril distance: straight-line distance from the posterior edge of the opening of the nostril to the anterior corner of the orbit (EN); tympanum diameter: the greatest horizontal distance between the outer edges of the tympanic annulus (TD); thumb length: straight line distance between the proximal edge of the prepollical tubercle and the end of the Finger I (FFL); Finger III length: straight-line distance between the proximal edge of the palmar tubercle and the end of Finger III (TFL); and disc width: the width of the terminal disc on Finger III (TFD). For a better understanding of how the measurements were taken see figure 5.1 in Duellman (2015). Comparative lengths of Fingers I and II were determined when adpressed against each other. Description of webbing follows Savage and Heyer (1967, 1997) with modifications of Myers and Duellman (1982). Specimens used for comparison and their associated locality data are listed in Appendix I.

We scanned the brooding female paratype of *Gastrotheca gemma* sp. nov. (CORBIDI 19396) on a SkyScan 1173 Micro-CT scanner at Instituto do Petróleo e dos Recursos Naturais (IPR). We set tube voltage and current at 60 kV and 75 μA, respectively, and voxel resolution was 25 μm. We visualized images using CT Vox 3.3.0 (Bruker MicroCT) and VG StudioMax (Volume Graphics, ver. 3.4.0). An image stack (TIFF) and 3D mesh files of the specimen were deposited in MorphoSource (doi:10.17602/M2/M160745). Cranial terminology follows Trueb (2015) and postcranial terminology follows Duellman and Trueb (1986) and Trueb (1973), manus and pes follow Fabrezi (1992, 1993, 2001), and ilium follows Gómez and Turazzini (2016).

Phylogenetics

We performed phylogenetic analyses in order to infer the phylogenetic position of *Gastrotheca gemma* sp. nov. within the genus. We used muscle tissue of the holotype (CORBIDI 21238) to sequence a fragment of 16S rRNA for *G. gemma* sp. nov. We extracted DNA with a commercial extraction kit (IBI Scientific, Peosta, USA). For the polymerase chain reaction (PCR) we used the 16Sar (forward) primer (5'-3' sequence: CGCCTGTTTATCA-AAAACAT) and the 16Sbr (reverse) primer (5'-3' sequence: CCGGTCTGAACTCAGATCACGT), and these thermocycling conditions: 1 cycle of 96 °C/3 min; 35 cycles of 95 °C/30 s, 55 °C/45 s, 72 °C/1.5 min; 1 cycle 72 °C/7 min (Palumbi et al. 2002). We ran the polymerase chain reaction (PCR) with a ProFlex thermal cycler (Applied Biosystems). We purified PCR products

with Exosap-IT Express (Affymetrix, Santa Clara, CA), and shipped the purified products to MCLAB (South San Francisco, CA) for sequencing.

We downloaded sequences of the following genes from GenBank DNA: 12S rRNA, 16S rRNA, NADH dehydrogenase subunit 1 (*ND1*), proopiomelanocortin A (*POMC*) and the recombination activating gene 1 (*RAG1*). We included terminals from all supraspecific clades currently considered for *Gastrotheca* (Echevarría et al. 2020). We used *Hemiphractus proboscideus* to root the tree. Terminals and GenBank accession numbers of DNA sequences used are listed in Appendix II.

We aligned sequences of each gene in Aliview 1.17.1 (Larsson 2014), using Muscle (Edgar 2004) with default parameters. We concatenated alignments into a single matrix and exported them in Nexus format using SequenceMatrix 1.7.8 (Vaidya et al. 2011). We assessed the best-fit partition scheme and models of evolution in PartitionFinder2 (Lanfear et al. 2017), under the corrected Akaike information criterion (AICc), as implemented on the Cipres Science Gateway (Miller et al. 2010). We evaluated the following partition schemes in the partition analysis: (i) unpartitioned, (ii) two partitions (by mitochondrial or nuclear gene category), (iii) five partitions (by gene). We conducted Maximum likelihood analyses using GARLI v2.01 (Zwickl 2006) as implemented on the Cipres Science Gateway. We set the analysis at 200 independent tree searches and 1,000 bootstrap pseudoreplicates. We set the genthreshfortopoterm (run termination threshold of generations without significant improvement in likelihood) at 100,000, and all other parameters as default. We used SumTrees 4.3.0 in DendroPy 4.3.0 (Sukumaran and Holder 2010) to summarize bootstrap pseudoreplicates. We used MEGA 7.0.14 (Kumar et al. 2016) to compute intraspecific uncorrected p-distances for the 16S rRNA (489 bp fragment).

To describe the results, we follow the taxonomy proposed by Echevarría et al. (2020).

Species concept

We considered multiple lines of evidence to support delimitation of the new species. For molecular analyses, we consider a species as the single lineage segment of ancestor-descendant populations or metapopulations evolving separately from other lineages (Simpson 1951; Wiley 1978; de Queiroz 1998; Wiley and Lieberman 2011). We used external morphological features to diagnose monophyletic groups inferred through phylogenetic analysis of DNA sequences.

Molecular assay for chytrid fungal infection

We used a real-time Polymerase Chain Reaction (PCR) assay on DNA material collected on skin swabs to quantify the level of *Bd* infection (Boyle et al. 2004). We extracted DNA from swabs using 40 ml of PrepMan Ultra,
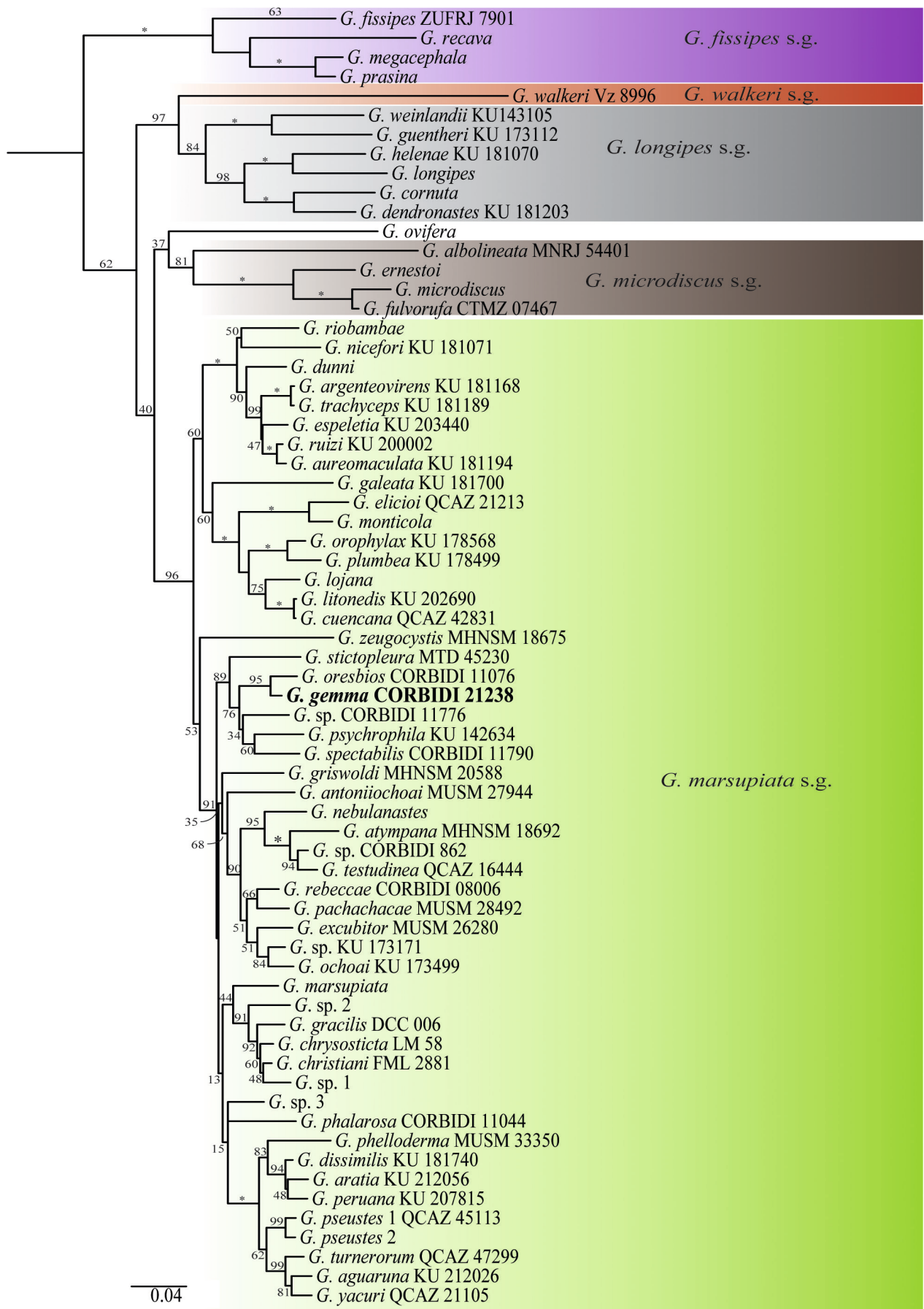
Figure 1. Maximum likelihood optimal tree (log likelihood = –36764.630331) inferred from 4,919 bp of mitochondrial (12S rRNA, 16S rRNA, ND1) and nuclear (POMC and RAG1) gene sequences. The phylogenetic tree depicts the relationships of *Gastrotheca gemma* sp. nov. with 67 *Gastrotheca* terminals, including 59 described species. Bootstrap support values of 100% are represented by an asterisk. Species groups are abbreviated as s.g.

and analysed extracts with a QuantStudio 3 qPCR system (ThermoFisher Scientific) following the protocol of Boyle et al. (2004) and Hyatt et al. (2007). We analysed each extract once. We calculated the number of zoospore equivalents ZE (i.e., the genomic equivalent for *Bd* zoospores) by comparing the qPCR results to a serial dilution of standards (gBlock synthetic standards, IDT DNA, Iowa, USA) and considered any sample with ZE >1 to be infected, or *Bd*-positive. We deposited the dataset of *Bd* prevalence and infection load at the online database https://amphibiandisease.org.

Results

The molecular dataset includes 68 terminals, 59 of which represent described species of *Gastrotheca*, and 4,919 aligned base pairs. According to the Partition-Finder results, we considered the five loci independently and applied the GTR + I + G model to each. The maximum likelihood optimal tree has a log likelihood score of –36764.630331 (Fig. 1). Bootstrap values are overall high. Among the main clades, the clade including *Gastrotheca ovifera* and the species groups of *G. marsupiata* and *G. microdiscus* has a low support value. The clade including G. ovifera as sister to the *G. microdiscus* species group has also low support.

The *Gastrotheca fissipes*, *G. longipes*, *G. marsupiata* and *G. microdiscus* species groups were recovered as monophyletic. Only one terminal of the *G. walkeri* species group was included. *Gastrotheca gemma* sp. nov. was recovered within the *Gastrotheca marsupiata* species group, as sister to *G. oresbios*. Other closely related species to *G. gemma* are: *G. psychrophila*, *G. spectabilis*, *G. stictopleura* and one undescribed species. The matrix of uncorrected p-distances for a 16S rRNA fragment shows that *G. oresbios* and *G. spectabilis* had the lowest distances with respect to *G. gemma* (Table 1).

Gastrotheca gemma sp. nov.

http://zoobank.org/195F5DAF-F4FD-4392-9CB5-A40B-3BA2805F

Figs. 2–6 and 8

Holotype. PERU • 1 ♀, a brooding adult; Amazonas department, Utcubamba province, Cajaruro district, from the trail from Refugio Lechucita to El Hito; 5°36'58.7''S, 78°14'58.8''W; 3180 m a.s.l.; 25 Nov. 2019; P.J. Venegas, L.A. García-Ayachi, J.C. Chávez-Arribasplata, J.R. Ormeño, S. Bullard and A. Marchelie leg.; CORBIDI 21238.

Paratypes (3). PERU • 1 ♀, adult; Amazonas department, Utcubamba province, Cajaruro district, from El Hito; 5°36'45.3''S, 78°15'2.9''W; 3300 m a.s.l.; 09 Nov. 2017; A. García-Bravo leg.; CORBIDI 19396 • 2 ♂, adults; Amazonas department, Utcubamba province, Cajaruro district, from Bosque Quemado; 5°36'8.5''S, 78°14'54.9''W; 3140 m a.s.l.; 28 Nov. 2019; P.J. Venegas, L.A. García-Ayachi, J.C. Chávez-Arribasplata, J.R. Ormeño, S. Bullard and A. Marchelie leg.; CORBIDI 21246–47.

Table 1. Uncorrected p-distances of the mitochondrial 16S rRNA gene between *Gastrotheca gemma* sp. nov. and closely related *Gastrotheca* species.

	1	2	3	4	5
1. *G. gemma* CORBIDI 21238					
2. *G. oresbios* CORBIDI 11076	2.3				
3. *G. psychrophila* KU 142634	5.2	5.2			
4. *G. spectabilis* CORBIDI 11790	4.5	4.8	4.3		
5. *G. stictopleura* MTD 45230	5.2	5.4	5.2	5.0	
6. *G.* sp. CORBIDI 11776	5.2	5.7	5.4	6.6	5.4

Referred specimens (3). CORBIDI 21239–41, three froglets that emerged from the dorsal brooding pouch of the holotype on 26 November 2019.

Diagnosis. Assigned to the genus *Gastrotheca* by females possessing a closed brood pouch on the dorsum. A moderately large species (69.7 and 71.8 mm SVL in two females, 56.9 and 59.5 mm SVL in two males), with: (1) tibia length 57–59% SVL, longer than foot; (2) interorbital distance greater than width of upper eyelid (161–169%); (3) skin on dorsum coarsely granular in females and granular in males, not co-ossified with skull, lacking transverse ridges; (4) supraciliary processes absent; (5) heel lacking calcar or tubercle; (6) tympanic annulus wrinkled or tuberculate; (7) Finger I slightly shorter than Finger II, width of discs wider than digits; (8) finger webbing present basally, only between III and IV; (9) foot webbing between external toes extending to nearly antepenultimate subarticular tubercle on Toe IV, to penultimate subarticular tubercle on Toe V; (10) in life, dorsum green with numerous minute black flecks in females and green with scattered yellow dots in males, paravertebral marks absent; (11) head markings consisting of a chocolate or pale green labial stripe in females and males, respectively; (12) dorsolateral stripe absent; (13) flanks uniformly green in females and green with numerous dark green irregular flecks in males; groin yellowish green in both sexes; anterior surfaces of thighs green, posterior surfaces of thighs yellowish green with scattered irregular black flecks in females and dense black reticulations in males; ventrolateral region yellowish green; irises silvery with a light blue hue or turquoise with thin black reticulations with or without an orange ring; (14) gular region and chest green in females and yellowish green in males; venter yellowish green with or without a big dark grey patch in the middle in females and venter greenish cream in males; ventral surface of thighs yellowish green with a dark greyish brown patch on the centre in females and thighs pale brownish cream in males; palms, soles and ventral surface of tarsus dark grey or dark greyish brown; (15) brood pouch single, dorsal; (16) reproduction mode direct development.

Gastrotheca gemma closely resembles *G. aguaruna*, *G. carinaceps*, and *G. dysprosita* from Peru, and *G. turnerorum* from Ecuador. *Gastrotheca gemma* shares with the aforementioned species a granular dorsal skin and a green dorsum, however the skin texture in *G. gemma* is coarsely granular, whereas it is weakly or finely granular in *G. aguaruna* and *G. carinaceps*, and granular in
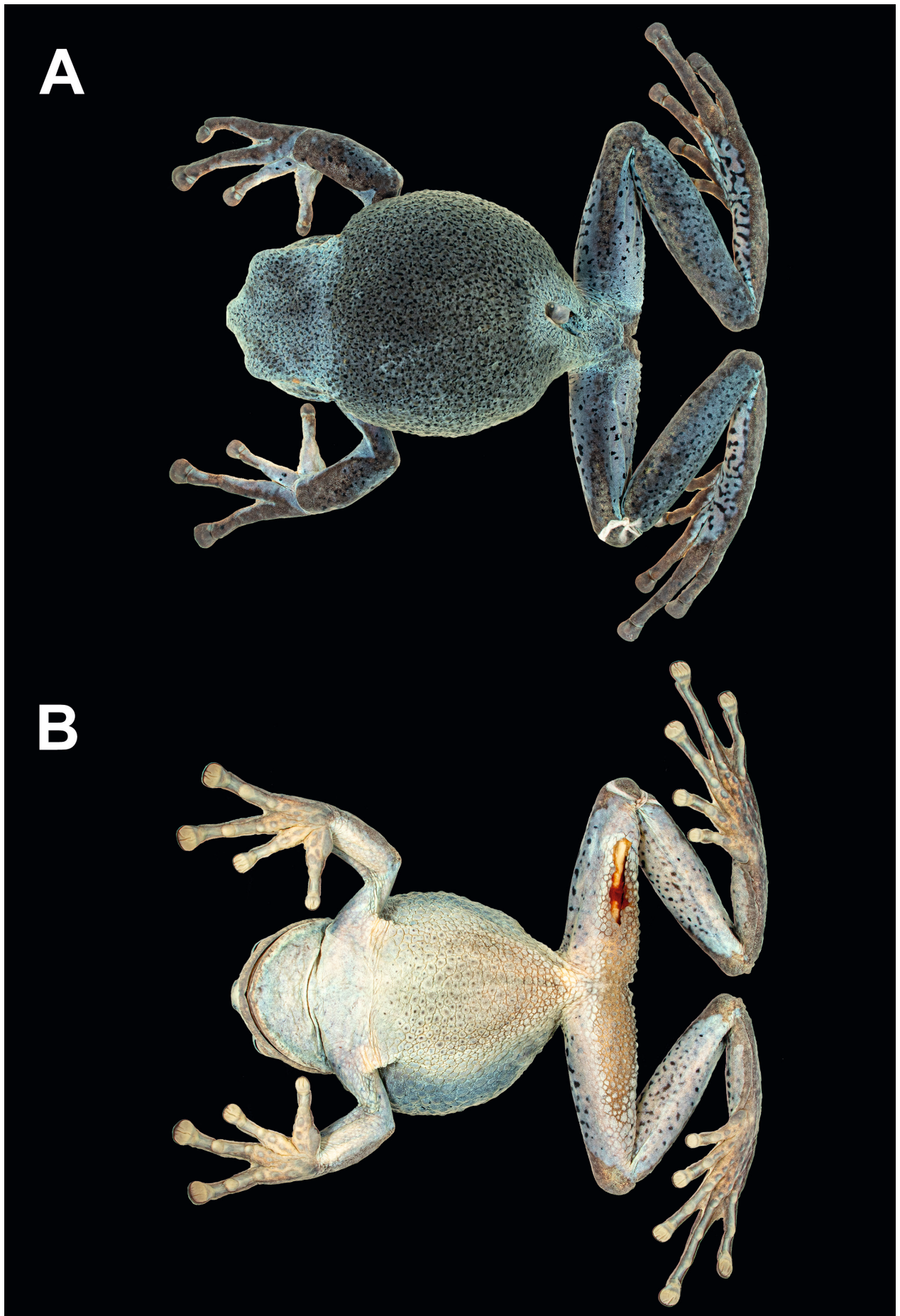
Figure 2. Preserved holotype of *Gastrotheca gemma* sp. nov. (CORBIDI 21238; female, SVL = 69.7 mm) in dorsal (A) and ventral (B) views.

Figure 3. Some morphological details of the preserved holotype of *Gastrotheca gemma* sp. nov.: dorsal (A) and lateral (B) views of the head, and views of palm (C) and sole (D). Scale bar 5 mm. Photographs by LAGA.

G. turnerorum. Furthermore, *G. aguaruna* differs by having finger I longer than II, and *G. carinaceps* finger I and II equal in size (finger I shorter than finger II in *G. gemma*). *Gastrotheca aguaruna* has a dorsolateral row of warts or tubercles, absent in *G. gemma*. *Gastrotheca turnerorum* also can be distinguished from *G. gemma* by having brown flanks and a dark brown venter with cream spots, while *G. gemma* has yellowish green flanks. The new species and *G. dysprosita* have a coarsely granular dorsum, however *G. dysprosita* differs from *G. gemma*

(character in parentheses) by having the interorbital distance smaller than width of upper eyelid (interorbital distance greater than width of upper eyelid), finger I and finger II equal in size (finger I shorter than finger II), dorsum with middorsal and dorsolateral stripes (dorsum without pattern), and venter cream with small brown spots (spots or blotches absent).

Gastrotheca gemma can be confused with green individuals of *G. monticola* and *G. ossilaginis* that also occur in the Andes of northern Peru (Duellman and Venegas

2005; Duellman et al. 2014). Nevertheless, *G. monticola* and *G. ossilaginis* have the dorsum finely shagreen (coarsely granular in *G. gemma*). Furthermore, *Gastrotheca monticola* differs from *G. gemma* by having the venter with scattered black spots (absent in the new species), and *G. ossilaginis* has the skin co-ossified with the skull (not co-ossified in *G. gemma*).

Phylogenetically, *G. gemma* is sister to *G. oresbios* and closely related to *G. psychrophila*, *G. spectabilis* and *G. stictopleura*. The skin on the dorsum of the adult female holotype of *G. oresbios*, the single known adult specimen of this species, was described as smooth with scattered tubercles (see Duellman and Venegas 2016). However, after the examination of the holotype of *G. oresbios*, we considered its skin texture shagreen with scattered tubercles, while in *G. gemma* is coarsely granular. Furthermore, *G. oresbios* has an acuminate snout in dorsal view and the dorsum tan with brown paravertebral marks (the new species possesses a rounded snout in dorsal view and green dorsum without marks). *Gastrotheca gemma* can be readily distinguished from *G. spectabilis*, *G. stictopleura* and *G. psychrophila* by differences in skin texture of dorsum: smooth in *G. spectabilis*, finely shagreen in *G. stictopleura* and granular in *G. psychrophila*; while in the new species is coarsely granular. *Gastrotheca spectabilis* has finger I equal in size to finger II whereas in the new species finger I is shorter than finger II. *Gastrotheca spectabilis* can be also distinguished from the new species by having a brown dorsum (dorsum green in *G. gemma*). *Gastrotheca stictopleura* is dorsally green, like *G. gemma*, but possesses a white dorsolateral stripe bordered below by brown (dorsolateral stripe absent in *G. gemma*). *Gastrotheca psychrophila* possess axilla, groins and hidden surfaces of hindlimbs blue or purple (yellowish green in *G. gemma*).

Gastrotheca gemma was found in syntopy with *G. abdita* in the páramo, however both can be easily distinguished by their skin texture, being smooth in *G. abdita*. Furthermore, the dorsum is usually brown with paravertebral stripes in *G. abdita*, but green in the new species. *Gastrotheca testudinea* also occurs in Cordillera de Colán but at lower elevations (from 1700 to 2200 m a.s.l.). *Gastrotheca testudinea* differs from the new species by having the dorsum smooth and finger I longer than finger II. Additionally, as in *G. abdita*, the dorsum of *G. testudinea* is usually brown.

Description of the holotype. An adult female (Fig. 2 and 3) in good state of preservation and with a piece of tissue removed from the left thigh for molecular analysis; SVL 69.7 mm; head wider than long; snout rounded in dorsal view, slightly inclined anteroventrally in profile; canthus rostralis round in section; loreal region slightly concave; lips rounded, broad; top of head granular; interorbital distance 173% of width of upper eyelid; internarial area flat; nostrils not protuberant, directed anterolaterally, to the level of anterior margin of lower jaw; diameter of eye is less than its distance from nostril; tympanum round, separated from the eye by a distance larger than the diameter of tympanum; tympanic annulus barely evident; supratympanic fold ill-defined, extending from behind the

Table 2. Measurements (in mm) of the type series of *Gastrotheca gemma* sp. nov.

	Gastrotheca gemma			
	21246♂	**21247♂**	**21238♀**	**19396♀**
SVL	57.0	59.5	69.7	71.8
TIBL	33.4	34.2	41.1	39.7
FL	31.8	30.5	37.7	35.6
HL	19.5	19.7	23.3	24.8
HW	24.2	24.6	27.2	27.8
IOD	8.0	8.8	9.7	10.1
EW	5.0	5.0	5.6	5.2
IND	3.7	3.7	3.9	4.1
ED	5.4	5.1	5.8	5.4
EN	5.4	5.9	7.2	6.7
TD	2.4	2.5	3.9	3.0
FFL	11.9	12.1	14.5	15.1
TFL	22.3	20.6	26.8	26.7
TFD	3.5	3.2	4.2	4.2

tympanum near to the insertion of the forelimb. Dentigerous vomerine processes narrowly separated medially, one bearing five teeth and the other six teeth.

Arm robust; ulnar tubercles absent; hand and fingers moderately large (TFL 38 % of SVL); fingers with basal web only between III and IV; discs large and rounded, width of disc of Finger III greater that diameter of tympanum; relative lengths of fingers I<II<IV<III; subarticular tubercles prominent, round in dorsal and profile views, none bifid; supernumerary tubercles, round; palmar tubercle ill-defined, bifid; prepollical tubercle large, elliptical. Hind limb robust; tibia length 59% of SVL; foot length 54% of SVL; calcar and tarsal tubercles absent; inner tarsal fold present; outer metatarsal tubercle absent; inner metatarsal tubercle elliptical, low; toes moderately long; relative length of toes I<II<III<V<IV; basal webbing between Toes I and II; webbing formula for other toes II1–2III1–2½IV2–1V; subarticular tubercles moderately large, rounded; supernumerary tubercles, numerous, and rounded; outer edge of toe V bears a fringe extending along the edge of foot.

Skin on dorsum coarsely granular; skin on flanks covered by enlarged flattened warts; skin on throat and chest weakly granular, ventral surfaces of thighs and arms coarsely granular; skin on belly granular; ventral surface of shanks smooth; two vertical rows of enlarged brown tubercles (three on left and two on right) below the cloacal opening. Tongue broad, suboval, not notched posteriorly, fully attached to mouth floor. Pouch opening V-shaped with anterior border at level of posterior edge of sacrum.

Measurements of the holotype (in mm). SVL: 69.7, TIBL: 41.1, FL: 37.7, HL: 23.3, HW: 27.2, IOD: 9.7, EW: 5.6, IND: 3.9, ED: 5.8, EN: 7.2, TD: 3.9, FFL: 14.5, TFL: 26.8, TFD: 4.2.

Colour of holotype. In life: dorsal surfaces green with numerous black flecks on dorsum, chocolate brown labial stripe, groins and ventrolateral region yellowish brown;
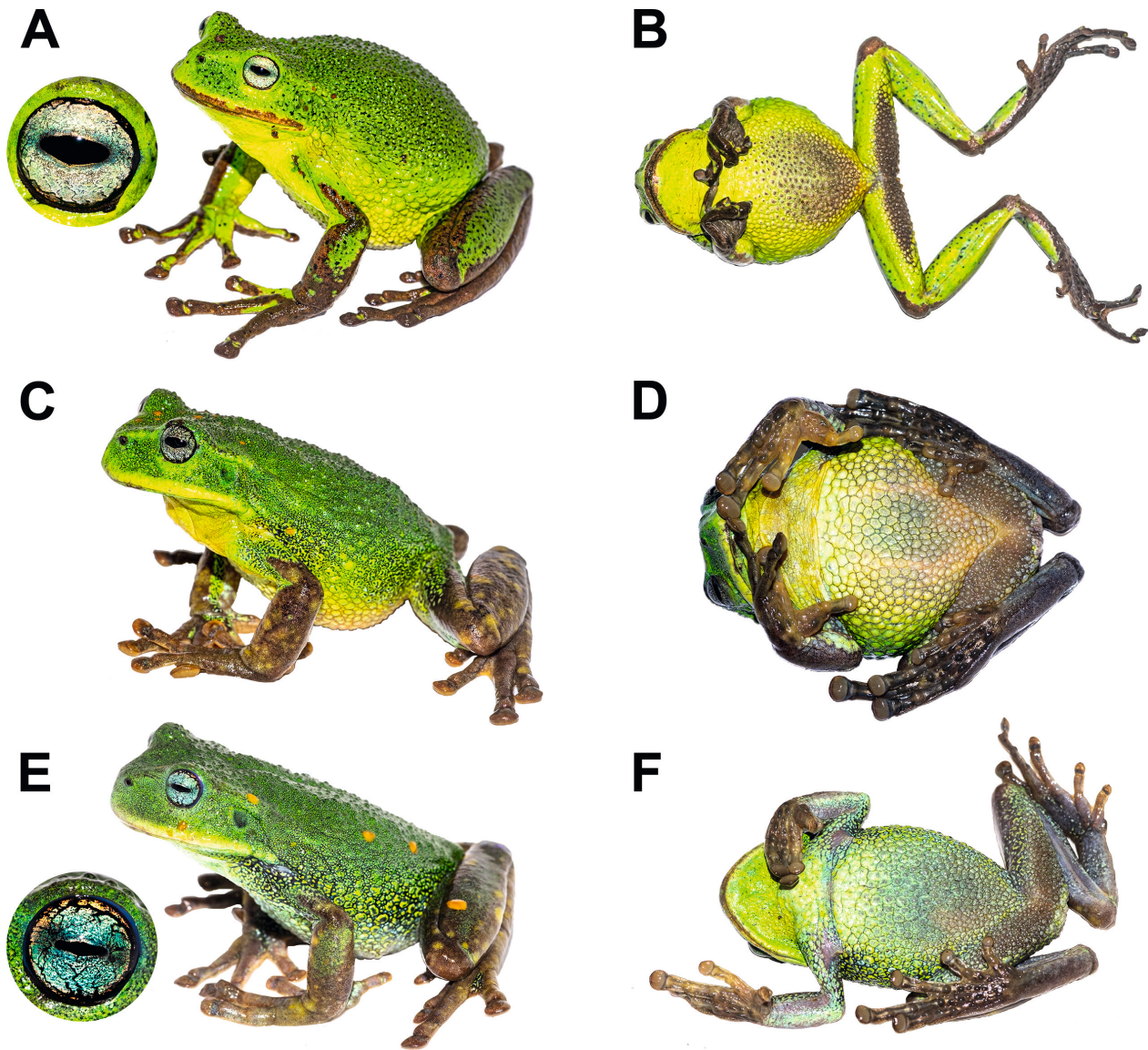
Figure 4. Three living adult specimens of *Gastrotheca gemma* sp. nov.: **(**A–B) dorsolateral and ventral views of female holotype (CORBIDI 21238), 69.7 mm SVL, with a zoom of its eye; (C–D) dorsolateral and ventral views of the adult male paratype (COR-BIDI 21246), 57.0 mm SVL; (E–F) dorsolateral and ventral views of the adult male paratype (CORBIDI 21247), 59.5 mm SVL, with a zoom of its eye. Photographs by AM.

forelimbs and fingers blotched with chocolate brown; hindlimbs with scattered black irregular flecks, numerous on shanks, larger on anterior surface of thighs, tarsus and feet; a chocolate brown stripe from the middle of thighs, running along knee, inner edge of shank and outer edge tarsus to toe V; toes chocolate brown. Ventral surface of throat, chest, forelimbs, belly and thighs yellowish green with a large greyish brown patch on the middle of the belly and a dark greyish brown patch on thighs; tibia and shanks green, ventral surface of tarsus, palms and soles dark greyish brown. Iris silvery with a light blue hue. In preservative (ethanol 70%): green coloration turns light blue and chocolate brown coloration turns pale brown on dorsal surface; ventrally, yellowish green coloration turns greyish light blue and dark greyish brown coloration turns light brown.

Intraspecific variation. Morphometric variation of two males and two females is summarized in Table 2. The single female paratype (CORBIDI 19396) is identical to the holotype varying only in lacking scattered black flecks on hindlimbs and the greyish patch in the middle of the belly, and by having turquoise irises. Females are larger than males (SVL in females 69.7–71.8 mm versus SVL in males 56.9–59.5 mm). However, *G. gemma* shows a strong sexual dimorphism in skin texture and coloration. Males have the skin on dorsum granular with scattered enlarged warts, while females have coarsely granular skin. In addition, have scattered large flattened warts on the dorsal surface of hindlimbs, whereas in females is smooth.

The dorsum in males (CORBIDI 21246–47; Fig. 4C–F) is green with scattered yellow dots, flanks green with numerous dark green irregular flecks, dorsal surface of hindlimbs greyish green with scattered yellow blotches,
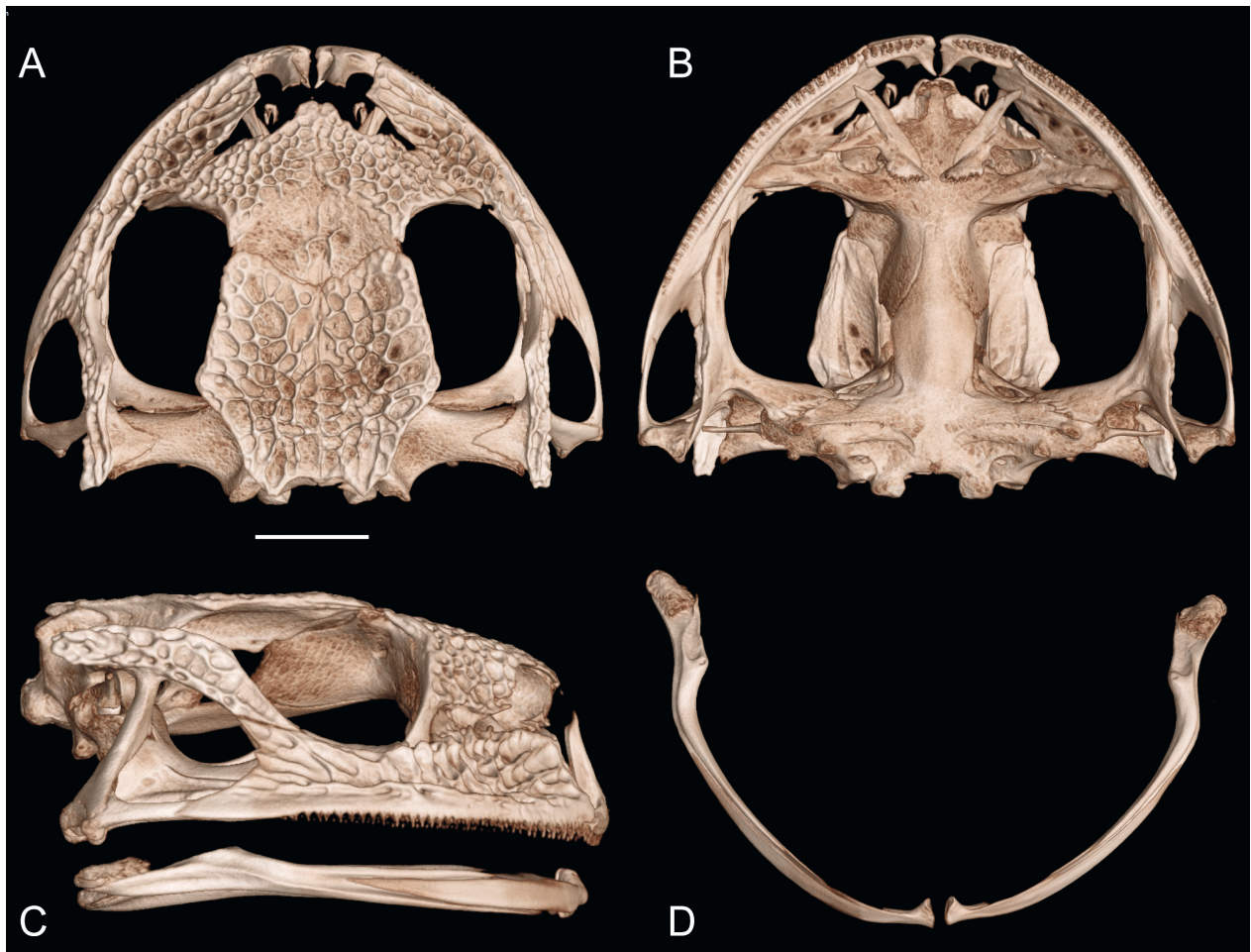
Figure 5. Skull of *Gastrotheca gemma* sp. nov. (CORBIDI 19396) as visualized via Micro-CT scanning in dorsal (A), ventral (B), and right lateral (C) views. (D) Mandible in dorsal view. Scale bar = 5 mm.

posterior surface of thighs yellow with a dense black reticulation, gular region yellow, venter greenish cream, and ventral surface of thighs pale greyish brown. Iris coloration in both male specimens were turquoise with thin black reticulations and with or without an orange ring (Fig. 4).

The froglets (CORBIDI 21239–41) have the skin on dorsal and ventral surfaces smooth. In life, the dorsal coloration is green, sides of head brown, limbs pale brown, venter yellow and the iris is bronze.

Osteology. Osteological description of a brooding female paratype of *Gastrotheca gemma* (CORBIDI 19396) with a SVL of 71.85 mm.

Cranial osteology. The skull of *Gastrotheca gemma* is wider than long and measures 22.7 mm in length from the jaw joint to the tip of the snout and 27.0 mm in width at the level of the quadratojugal. The skull is hyperossified, with well-developed pit-and-ridge dermal sculpturing (i.e., exostosis) on the frontoparietals, squamosals, maxillae, and nasals (Fig. 5A). The exposed sphenethmoid has irregular vermiform ridging. The frontoparietals have a complete medial articulation with one another, and a moderately wide supraorbital and otic flange is present but does not form an articulation with the head of the squamosal (and

therefore a temporal arcade is absent). The frontoparietal covers the anterior epiotic eminence, and the carotid canal is partially closed. The nasals are expanded, articulating with the pars facialis of the maxilla, and form a bony anterior orbital margin. The nasals overlap the anterior margin of the sphenethmoid and extend posteriorly but do not articulate with the anterior edges of the frontoparietal. The maxillary arcade is complete. The quadratojugal is broadly overlapped laterally by the maxilla. The large postorbital process of the maxilla articulates with the zygomatic ramus of the squamosal via a broad diagonal articulation, forming the posterior margin of the orbit (Fig. 5C). The head of the squamosal has a moderately wide crest, and the otic plate of the squamosal covers 35% of the width of the crista parotica. The zygomatic ramus of the squamosal bifurcates distally, and the medial branch articulates with a high dorsal process of the anterior ramus of the pterygoid and the lateral branch articulates with the pars facialis of the maxilla. The anterior ramus of the pterygoid articulates with the lingual edge of the pars palatina of the maxilla. The premaxillae are broad and bear alary processes that are deflected posteriorly at a 25° angle, forming a high and slightly rounded snout in lateral profile. The palate is characterized by well-developed neopalatines that are widely separated from one another and form a posterior margin to the choana (Fig. 5B). The prechoanal processes of the
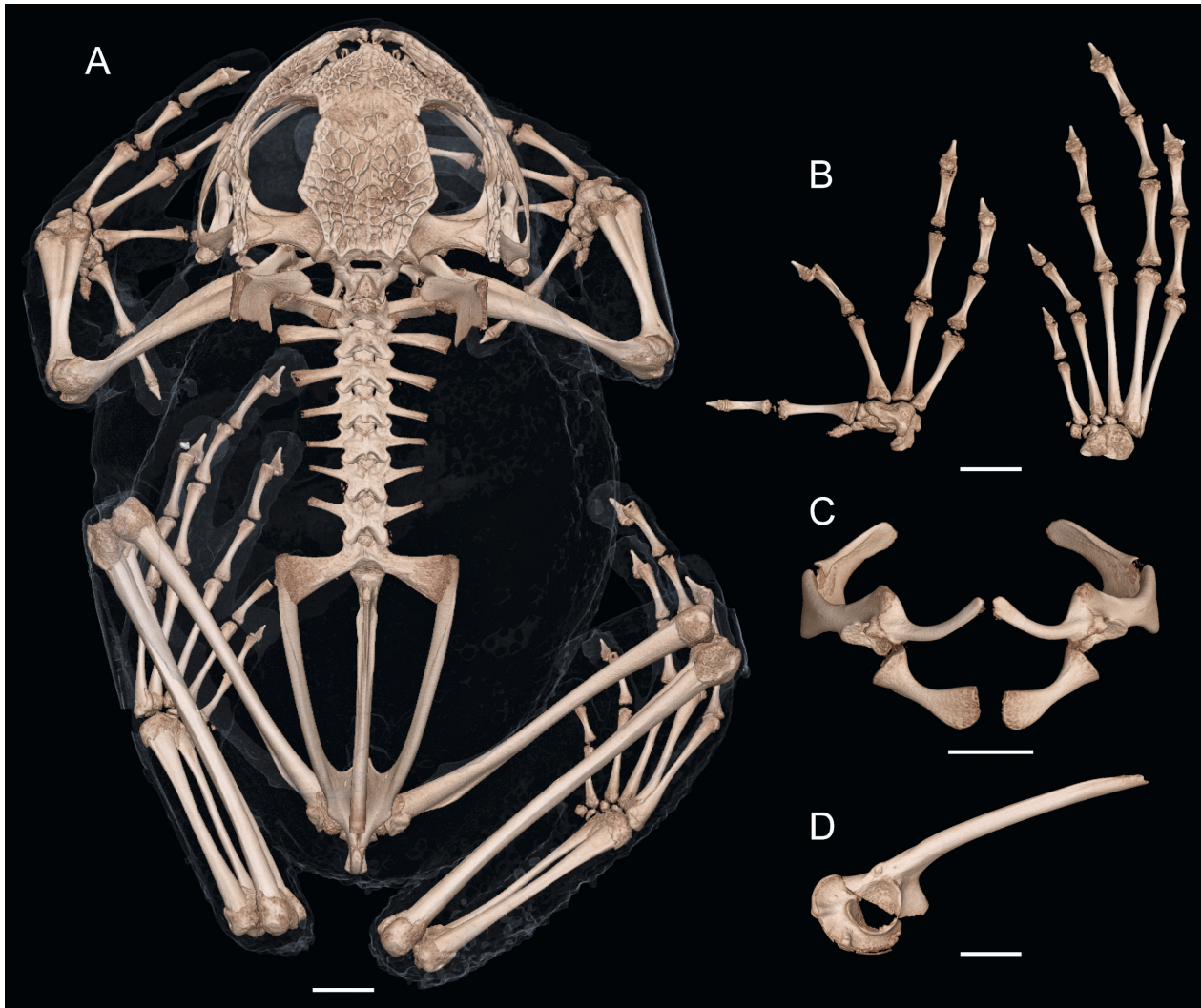
Figure 6. Skeleton of *Gastrotheca gemma* sp. nov. (CORBIDI 19396) as visualized via Micro-CT scanning in dorsal view (A). (B) Left manus and pes in ventral view, (C) pectoral girdle in ventral view, and (D) ilium in right lateral view. Scale bar = 5 mm.

vomers are long and articulate with the lingual surface of the pars facialis of the maxilla and the neopalatines, supporting the complete anterior margin of the choana. The postchoanal processes of the vomers are short and support half of the medial choanal margin. The dentigerous processes of the vomers are located at the level between the posterior portions of the choanae. The parasphenoid is synostosed to the overlying prootics and exocciptials. The cultriform process narrows abruptly anterior to the optic fenestra and terminates posterior to the level of the neopalatines. The sphenethmoid is not synostosed with the prootic. There are 30 to 42 socketed, pedicellate teeth on each maxilla, 7 to 10 teeth on each premaxilla, and 5 teeth on each vomer. The dentary is edentate (Fig. 5D).

Postcranial osteology. *Vertebral column*. Eight presacral vertebrae, the low neural spines of the atlas and presacral II articulate while the remaining presacrals are non-imbricate (Fig. 6A). Neural arches of presacrals III–VIII lack neural spines. The atlas lacks transverse processes, presacrals II–IV bear thicker and longer processes than presacrals V–VIII. The transverse processes of presacral III are expanded distally, those of presacrals II and IV

are slightly expanded distally. The transverse process of presacrals II and VIII are anteriorly directed, those of presacrals III, VI and VII are perpendicular to the notochordal axis, and those of presacrals IV and V are posteriorly directed. Lengths of the transverse process of presacrals along with that of the sacral diapophyses (SD): SD > III > II > IV > V–VII > VIII. The anterior margin of the sacral diapophyses is perpendicular to the longitudinal axis of the vertebra column. The distal ends of sacral diapophyses are expanded, approximately twice the width of the base. Both anterior and posterior margins of the sacral diapophyses are straight. The lateral margins are convex. The urostyle is as long as the presacral portion of the vertebral column and has a bicondylar articulation with the sacrum. The shaft of the urostyle is dorsoventrally compressed in cross section. The width of the shaft of the urostyle is narrow anteriorly. The urostyle bears a dorsal crest along half of the bone shaft, the crest is higher anteriorly and gradually diminishes in height posteriorly.

Pectoral girdle. Arciferal pectoral girdle (Fig. 6C). Clavicles curved and concave. Clavicles are uniform in width, only the lateral region is wider. Laterally each clavicle is

fused to the pars acromialis of the scapula. Medial tips of clavicles not in contact, reaching to the level of the antero-lateral end of each clavicle. The clavicles do not reach the glenoid fossa. In ventral view, the sternal and glenoid ends of the coracoids have the same width and the midshaft has half the width of the lateral ends. The sternal end is flattened and the glenoid end is wide and slightly concave. The sternal ends of the coracoids are not in contact. The scapula is stout, longer than the coracoid. The pars glenoidalis is narrower than the pars acromialis. The suprascapular end is narrower than the zonal end. The coracoid and scapula form the margin of the glenoid fossa. Cleithrum and ossified portion of the suprascapula fused.

Pelvic girdle. In dorsal view, the ilial shafts have a V–shaped configuration. The ilial shaft has a low dorsal crest (Fig. 6D). The dorsal prominence is low but conspicuous, the associated dorsal protuberance is elongate, conspicuous and positioned above the dorsal margin of the acetabular fossa. The ventral anterior margin of the ventral acetabular expansion is straight and forms an angle of approximately 90° with the ilial shaft. The articulations of the ilium with the ischium and pubis are evident, but not the articulation of the pubis and the ilium.

Forelimb and manus. The humerus has a prominent ventral crest, extending along more than half the length of the bone, higher at the proximal end of the humerus and gradually diminishing in height distally. The distal head (eminentia capitata) is expanded and it is wider than the glenoid head (caput humeri). The radioulna is flattened and distinctly wide distally; the sulcus intermedius is indicated by a distinct groove on the distal half of the bone. The carpus is composed by radiale, ulnare, distal carpal 5–4–3, element Y fused to distal carpal 2, and elements of the prepollex. The phalangeal formula is 2–2–3–3 (Fig. 6B). The terminal phalanges have a rounded proximal base, from the base towards the tip become gradually narrower. The prepollex has two elements, including the base.

Hind limb and pes. The femur is slightly sigmoid, shorter than the tibiofibula. The sulcus intermedius of the tibiofibula is shallow. The tibiale and fibulare are separated medially and fused at the proximal and distal ends. These bones are approximately half the length of the tibiofibula. There are four tarsal elements: element Y, two distal tarsals, and the prehallux. The element Y articulates with the prehallux. There is a single ossified element of the small prehallux. The phalangeal formula is 2–2–3–4–3 (Fig. 6B). The terminal phalanges have a rounded proximal base, from the base towards the tip become gradually narrower.

Distribution and natural history. *Gastrotheca gemma* is only known from three close localities on the summit of the Cordillera de Colán, at elevations from 3130 to 3180 m a.s.l. (Fig. 7). The three close known localities for this species lay in the Peruvian Yunga ecoregion according to Olson et al. (2001). The localities of El Hito and Bosque Quemado are within the Santuario Nacional

Cordillera de Colán, a natural reserve protected by the Peruvian government (Fig. 7). The new species inhabits the páramo and the ecotone between páramo and humid montane forest. We found the holotype, a brooding female, basking at 1400 hours on 25 November 2019 on top of a bush at 1.5 m above the ground, in a scrub patch with *Chusquea* spp. (Poaceae) at the border of a summit covered by páramo vegetation. At El Hito we found another brooding female (CORBIDI 19396) at 1200 hours on 9 October 2017 during a cloudy day, perched on Stipa grass (*Stipa* sp.). We found the two male paratypes at night (1900 hours) on a patch of spiny ground bromeliads in a swamp area full of scrubs and *Chusquea* spp.

Syntopic species include *G. abdita*, *Pristimantis atrabracus*, *P. corrugatus*, *P.* sp. and *Ctenophryne* sp. Three completely developed froglets emerged from the holotype's dorsal pouch during the photographic session. All froglets were similar in size (SVL between 11.30 and 11.33 mm). One paratype (CORBIDI 19396) is a brooding female with 34 embryos in her pouch (Fig. 8).

We did not detect infection by the fungal pathogen *Batrachochytrium dendrobatidis* (*Bd*) in the three sampled specimens of *G. gemma* (CORBIDI 21238, 21246–47), but *Bd* prevalence among syntopic frogs was 10.2% (Bayes 95% credible interval with Jeffrey's priors: 3.7–18.7%). Among six infected frogs, only one had ZE > 10,000, a threshold known to be associated with elevated mortality (Kinney et al. 2011; Catenazzi et al. 2017): *G. abdita* CORBIDI 21281 had ZE = 12,904 zoospore equivalents. Overall, *Bd* prevalence and infection loads were low compared to other frog assemblages in the high Andes (Catenazzi and von May 2014).

Etymology. The specific epithet comes from the Latin word "*gemma*", a substantive meaning precious stone or gem. This specific name is used in apposition and refers to the turquoise coloration, in life, of the eyes of the new species of marsupial frog, which resembles the coloration of a turquoise stone.

Discussion

The description of *Gastrotheca gemma* increases the number of *Gastrotheca* species reported from Peru to 31, among these 26 are endemic. *Gastrotheca gemma* is the second species of the genus described from Cordillera de Colán. The LSU ornithological expedition collected *G. abdita*, also a direct-developer, more than 40 years ago. This poorly known species was considered the only *Gastrotheca* species inhabiting Cordillera de Colán. Duellman (2015) tentatively identified a juvenile *Gastrotheca* (CORBIDI 862) from Cordillera de Colán as *G. abdita*. We examined this juvenile specimen and observed characteristics in disagreement with the diagnosis of *G. abdita*, but in agreement with the diagnosis of *G. testudinea*. In support of this identification, the uncorrected p-distances for a 16S rRNA fragment between *G.* sp. CORBIDI
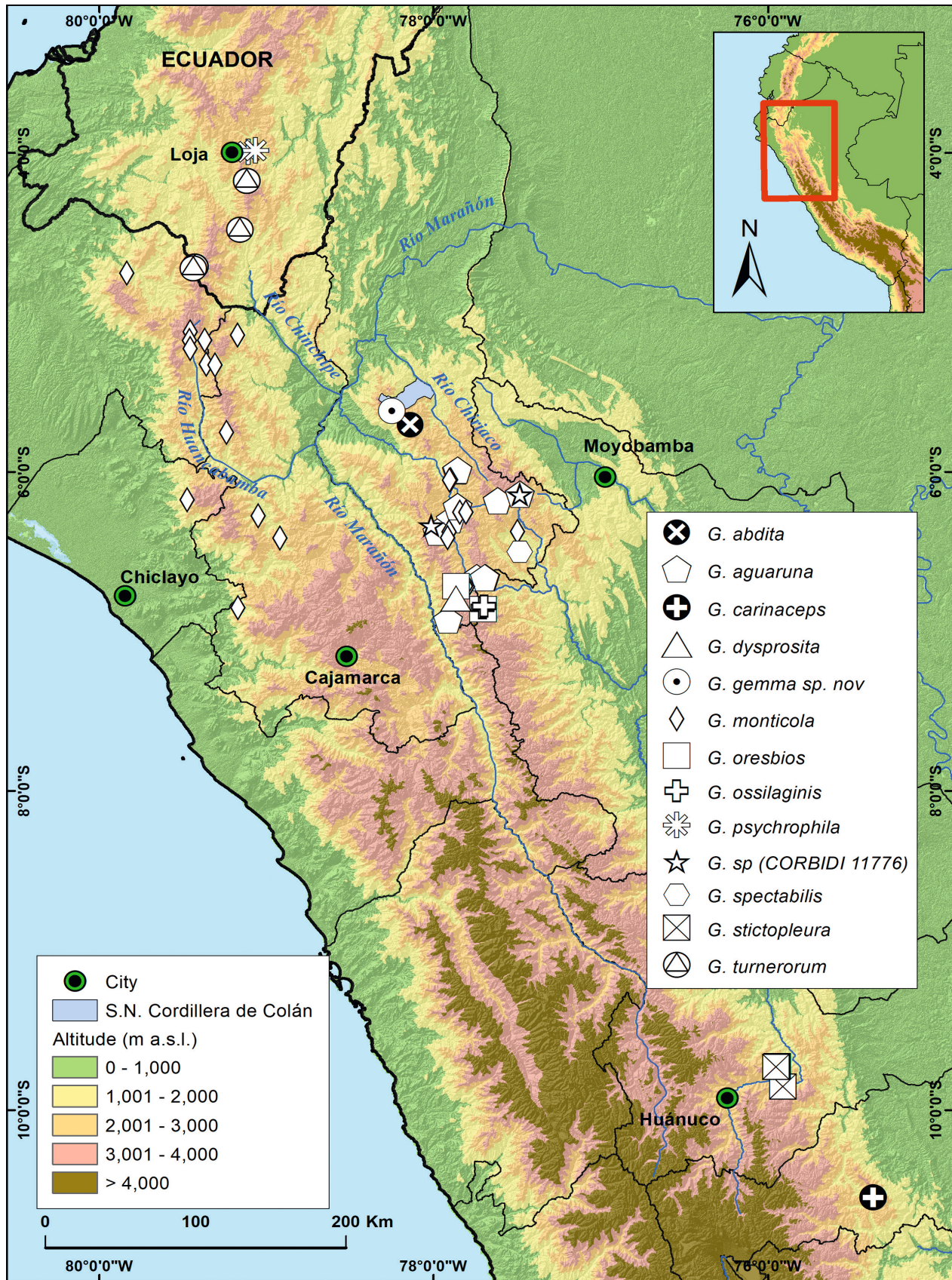
Figure 7. Geographical distribution of *Gastrotheca gemma* sp. nov. and closely related and similar species from Ecuador and Peru.

862 and *G. testudinea* QCAZ 16444 is 1.8% (Table 1). During the recent field expeditions to Cordillera de Colán we collected both *G. testudinea* and *G. abdita*, however *G. testudinea* was never found above 2200 m a.s.l.

The cranial morphology of *Gastrotheca* is morphologically complex, particularly in the Andean clade *Gastrotheca marsupiata* species group. *Gastrotheca galeata* possesses a highly derived, casqued skull that bears little
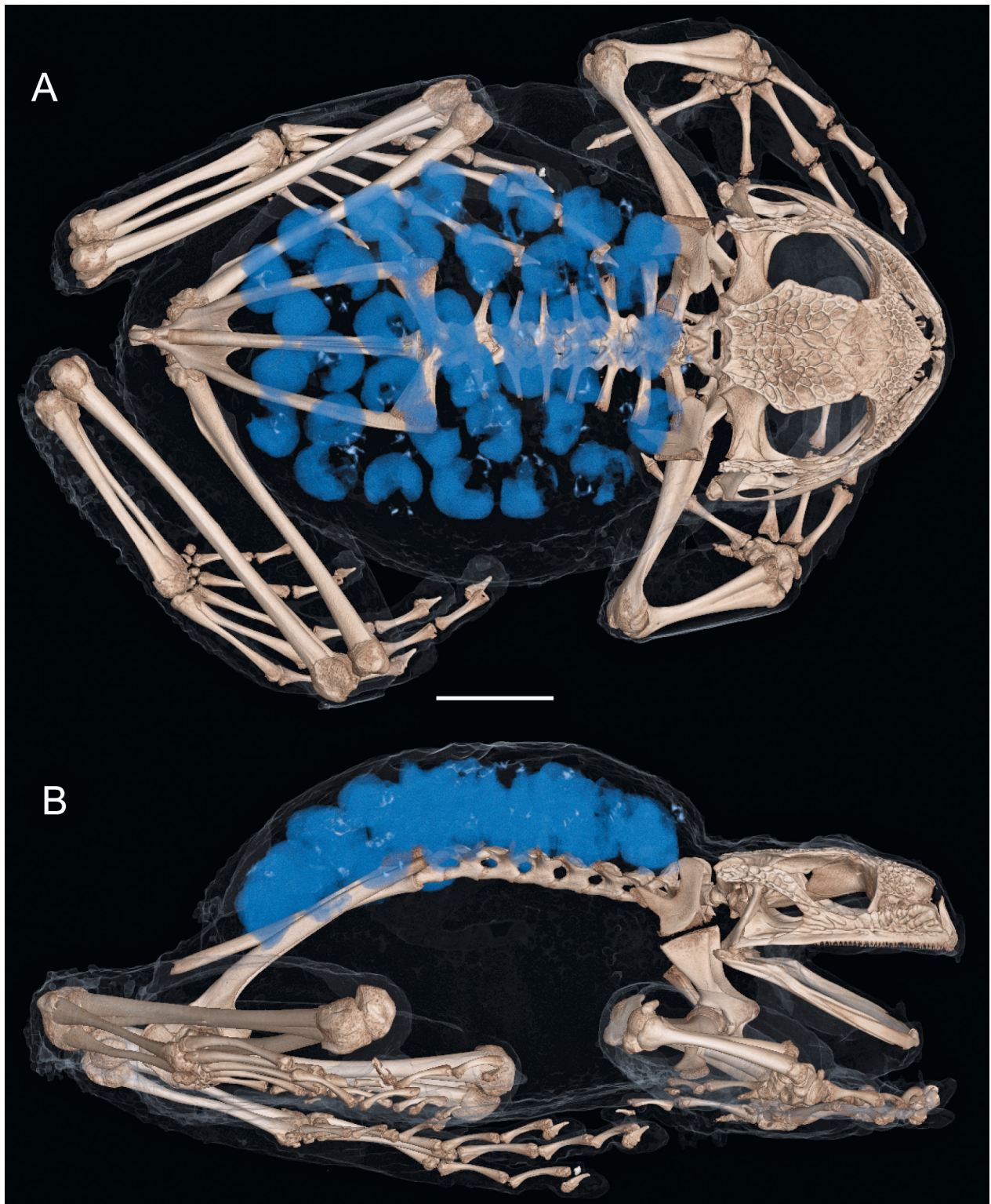
Figure 8. Skeleton and 34 embryos in pouch of *Gastrotheca gemma* sp. nov. (CORBIDI 19396) as visualized via Micro–CT scanning in dorsal (A) and right lateral (B) views. (A) Scale bar = 10 mm.

similarity to other species in the genus due to a unique sculpturing pattern and extensive synostosis (Trueb and Duellman 1978; Duellman 2015) and is more similar in skull shape to distantly related anurans known to use phragmotic behaviour (e.g., *Smilisca fodiens*, *Peltophryne* toads; Paluh et al. 2020). Species in the *Gastrotheca marsupiata* species group are highly variable and challenging to morphologically characterize (Duellman

2015). For example, variation exists across Andean *Gastrotheca* in the presence or absence of dermal sculpturing, supraorbital and otic flanges, a temporal arcade, and articulation between the zygomatic ramus of the squamosal and maxilla, prominently altering the overall architecture of the skull. The amount of homoplasy in these characters has not been investigated but is likely high. *Gastrotheca gemma* was recovered within a clade that includes

G. oresbios, *G. psychrophila*, *G. spectabilis*, and *G. stictopleura*. Of these closely related species, the skull anatomy has been described for only *G. psychrophila* (Duellman 2015). *Gastrotheca gemma* and *G. psychrophila* share several cranial characters, including the presence of wide supraorbital and otic flanges, a frontoparietal that covers the anterior epiotic eminence, a partially closed carotid canal, alary processes of the premaxillae that are deflected posteriorly, and the absence of a temporal arcade. *Gastrotheca psychrophila* differs from *G. gemma* in that the sphenethmoid is hyperossified with pit-and-ridge sculpturing and the nasals articulate with the anterior edges of the frontoparietal. The postcranial osteology of *Gastrotheca* has been less extensively studied, there are descriptions for *G. carinaceps*, *G. galeata*, *G. lateonota* and *G. monticola* (Duellman and Trueb 1978, 1988; Duellman et al. 2006). The presacral and sacral regions and ilium of *G. gemma* is very similar to those of the aforementioned members of the *G. marsupiata* species group. The clavicles are curved and robust as in *G. lateonota* and *G. monticola*. As stated by Duellman et al. (2006) the postcranial osteology, among these few species of the *G. marsupiata* species group, seems relatively conserved.

The herpetofauna of the isolated Cordillera de Colán deserves further investigation, in fact the expedition in which *G. gemma* was discovered is one of three expeditions targeting exclusively the unknown diversity of this group.

Acknowledgments

References

Blackburn DC, Duellman WE (2013) Brazilian marsupial frogs are diphyletic (Anura: Hemiphractidae: *Gastrotheca*). Molecular Phylogenetics and Evolution 68: 709–714.

Boyle DG, Boyle DB, Olsen V, Morgan JAT, Hyatt AD (2004) Rapid quantitative detection of chytridiomycosis (*Batrachochytrium dendrobatidis*) in amphibian samples using real-time Taqman PCR assay. Diseases of Aquatic Organisms 60: 141–148.

Burkart D, Flechas SV, Vredenburg VT, Catenazzi A (2017) Cutaneous bacteria, but not peptides, are associated with chytridiomycosis resistance in Peruvian marsupial frogs. Animal Conservation 20: 483–491.

Castroviejo-Fisher S, De La Riva I, Pombal Jr JP, da Silva HR, Rojas-Runjaic FJM, Medina-Méndez E, Frost DR (2015) Phylogenetic systematics of egg-brooding frogs (Anura: Hemiphractidae) and the evolution of direct development. Zootaxa 4004: 1–75.

Catenazzi A, von May R (2014) Conservation status of amphibians in Peru. Herpetological Monographs 28: 1–23.

Catenazzi A, Lehr E, Vredenburg VT (2014) Thermal physiology, disease, and amphibian declines on the eastern slopes of the Andes. Conservation Biology 28: 509–517.

Catenazzi A, Lehr E, Rodriguez LO, Vredenburg VT (2011) *Batrachochytrium dendrobatidis* and the collapse of anuran species richness and abundance in the upper Manu National Park, southeastern Peru. Conservation Biology 25: 382–391.

Catenazzi A, Swei A, Finkle J, Foreyt E, Wyman L, Vredenburg VT (2017) Epizootic to enzootic transition of a fungal disease in tropical Andean frogs: Are surviving species still susceptible?. PLoS One 12: e0186478.

de Queiroz K (1998) The general lineage concept of species, species criteria, and the process of speciation. In Howad DJ, Berlocher SH (Eds) Endless forms: species and speciation. Oxford University Press, New York, 57–75.

Duellman WE (2015) Marsupial frogs: *Gastrotheca* and allied genera. Johns Hopkins University Press, Baltimore, 407 pp.

Duellman WE, Trueb L (1978) An extraordinary new casque-headed marsupial frog (Hylidae: *Gastrotheca*). Copeia 1978: 498–503.

Duellman WE, Trueb L (1986) Biology of amphibians. Johns Hopkins University Press, Baltimore, 671 pp.

Duellman WE, Trueb L (1988) Cryptic species of hylid marsupial frogs in Peru. Journal of Herpetology 22: 159–179.

Duellman WE, Hillis DM (1987) Marsupial frogs (Anura: Hylidae: *Gastrotheca*) of the Ecuadorian Andes: resolution of taxonomic problems and phylogenetic relationships. Herpetologica 1987: 141–173.

Duellman WE, Pramuk JB (1999) Frogs of the genus *Eleutherodactylus* (Anura: Leptodactylidae) in the Andes of northern Peru. Scientific Papers Natural History Museum The University of Kansas 13: 1–78.

Duellman WE, Venegas P (2005) Marsupial frogs (Anura: Hylidae: *Gastrotheca*) from the Andes of northern Peru with descriptions of two new species. Herpetologica 61: 295–307.

Duellman WE, Venegas PJ (2016) Diversity of marsupial frogs (Anura: Hemiphractidae: *Gastrotheca*) in the northern Cordillera Central, Peru, with the descriptions of two new species. Phyllomedusa 15: 103–117.

Duellman WE, Trueb L, Lehr E (2006) A new species of marsupial frog (Anura: Hylidae: *Gastrotheca*) from the Amazonian slopes of the Cordillera Oriental in Peru. Copeia 2006: 595–603.

Duellman WE, Barley AJ, Venegas PJ (2014) Cryptic species diversity in marsupial frogs (Anura: Hemiphractidae: *Gastrotheca*) in the Andes of northern Peru. Zootaxa 3768: 159–177.

Echevarría LY, De la Riva I, Venegas PJ, Rojas-Runjaic FJM, Dias IR, Castroviejo-Fisher S (2020) Total evidence and sensitivity phylogenetic analyses of egg-brooding frogs (Anura: Hemiphractidae). Cladistics 2020: 1–27.

Edgar RC (2004) MUSCLE: a multiple sequence alignment method with reduced time and space complexity. BMC Bioinformatics 5: 113.

Fabrezi M (1992) El carpo de los anuros. Alytes 10: 1–29.

Fabrezi M (1993) The anuran tarsus. Alytes 11: 47–63.

Fabrezi M (2001) A survey of prepollex and prehallux variation in anuran limbs. Zoological Journal of the Linnean Society 131: 227–248.

Frost DR (2020) Amphibian Species of the World: an Online Reference. Version 6.1. https://amphibiansoftheworld.amnh.org/index.php [Accessed 10 Jul. 2020]

Gómez RO, Turazzini GF (2016) An overview of the ilium of anurans (Lissamphibia, Salientia), with a critical appraisal of the terminology and primary homology of main ilial features. Journal of Vertebrate Paleontology 36: e1030023.

Hyatt DG, Boyle AD, Olsen V, Boyle DB, Berger L, Obendorf D, Phillott R (2007) Diagnostic assays and sampling protocols for the detection of *Batrachochytrium dendrobatidis*. Diseases of Aquatic Organisms 73: 175–192.

Kinney VC, Heemeyer JL, Pessier AP, Lannoo MJ (2011) Seasonal pattern of *Batrachochytrium dendrobatidis* infection and mortality in *Lithobates areolatus*: Affirmation of Vredenburg's "10,000 Zoospore Rule". PLoS One 6: e16708.

Kumar S, Stecher G, Tamura K (2016) MEGA7: Molecular Evolutionary Genetics Analysis Version 7.0 for Bigger Datasets. Molecular Biology and Evolution 33: 1870–1874.

Lanfear R, Frandsen PB, Wright AM, Senfeld T, Calcott B (2017) PartitionFinder 2: new methods for selecting partitioned models of evolution for molecular and morphological phylogenetic analyses. Molecular Biology and Evolution 34: 772–773.

Larsson A (2014) AliView: a fast and lightweight alignment viewer and editor for large datasets. Bioinformatics 30: 3276–3278.

Lehr E, Catenazzi A (2011) A new species of marsupial frog (Anura: Hemiphractidae: *Gastrotheca*) from the Río Abiseo National Park in Peru. Herpetologica 67: 449–459.

Miller MA, Pfeiffer W, Schwartz T (2010) Creating the CIPRES Science Gateway for inference of large phylogenetic trees. In Gateway Computing Environments Workshop (GCE), New Orleans, 1–8.

Myers CW, Duellman WE (1982) A new species of *Hyla* from Cerro Colorado, and other tree frog records and geographical notes from western Panama. American Museum Novitates 2752: 1–32.

Olson DM, Dinerstein E, Wikramanayake ED, Burgess ND, Powell GVN, Underwood EC, Kassem KR (2001) Terrestrial Ecoregions of the World: A new Map of Life on Earth. BioScience 51: 933–938.

Paluh DJ, Stanley EL, Blackburn DC (2020) Evolution of hyperossification expands skull diversity in frogs. Proceedings of the National Academy of Sciences 117: 8554–8562.

Palumbi S, Martin A, Romano S, McMilan WO, Stice L, Grabowski G (2002) Simple fool's guide to PCR: Version 2.0. Department of Zoology and Kewalo Marine Laboratory, University of Hawaii, 45 pp.

Rivera-Correa M, Garcia-Burneo K, Grant T (2016) A new red–eyed of stream treefrog *Hyloscirtus* (Anura: Hylidae) from Peru, with comments on the taxonomy of the genus. Zootaxa 4061: 29–40.

Rodriguez LO, Catenazzi A (2017) Four new species of terrestrial-breeding frogs of the genus *Phrynopus* (Anura: Terrarana: Craugastoridae) from Río Abiseo National Park, Peru. Zootaxa 4273: 381–406.

Savage JM, Heyer WR (1967) Variation and distribution in the treefrog genus *Phyllomedusa* in Costa Rica, central America: Studies on Neotropical Fauna and Environment 5: 111–131.

Savage JM, Heyer WR (1997) Digital webbing formulae for anurans: a refinement. Herpetological Review 28: 131.

Scheele BC, Pasmans F, Skerratt LF, Berger L, Martel AN, Beukema W, Acevedo AA, Burrowes PA, Carvalho T, Catenazzi A, De la Riva I, Fisher MC, Flechas SV, Foster CN, Frías-Álvarez P, Garner TWJ, Gratwicke B, Guayasamin JM, Hirschfeld M, Kolby JE, Kosch TA, La Marca E, Lindenmayer DB, Lips KR, Longo AV, Maneyro R, McDonald CA, Mendelson III J, Palacios-Rodriguez P, Parra-Olea G, Richards-Zawacki CL, Rödel M-O, Rovito SM, Soto-Azat C, Toledo LF, Voyles J, Weldon C, Whitfield SM, Wilkinson M, Zamudio KR, Canessa S (2019) Amphibian fungal panzootic causes catastrophic and ongoing loss of biodiversity. Science 363: 1459–1463.

Simpson GG (1951) The species concept. Evolution 5: 285–298.

Sukumaran J, Holder MT (2010) DendroPy: a Python library for phylogenetic computing. Bioinformatics 26: 1569–1571.

Trueb L (1973) Bones, frogs, and evolution. In Vial JL (Eds) Evolutionary biology of the anurans: contemporary research on major problems. University of Missouri Press, Missouri, 65-132.

Trueb L (2015) Osteology. In Duellman WE (Eds) Marsupial frogs: *Gastrotheca* and allied genera. Johns Hopkins University Press, Baltimore, 31–51.

Trueb L, Duellman WE (1978) An extraordinary new casque-headed marsupial frog (Hylidae: *Gastrotheca*). Copeia 1978: 498–503.

Vaidya G, Lohman DJ, Meier R (2011) SequenceMatrix: concatenation software for the fast assembly of multi-gene datasets with character set and codon information. Cladistics 27: 171–180.

Venegas PJ, Barrio J (2005) A new species of harlequin frog (Anura: Bufonidae: *Atelopus*) from the northern Cordillera Central, Peru. Revista Española de Herpetología 29: 103–112.

Wiley EO (1978) The evolutionary species concept reconsidered. Systematic Zoology 27: 17–26.

Wiley EO, Lieberman BS (2011) Phylogenetics: Theory and practice of phylogenetic systematics: John Wiley and Sons, New Jersey, 431 pp.

Zwickl DJ (2006) Genetic algorithm approaches for the phylogenetic analysis of large biological sequence datasets under the maximum likelihood criterion. Doctor of Philosophy Thesis, The University of Texas, Austin.

Appendix 1

Examined specimens

Gastrotheca aguaruna — PERU: **Amazonas**: Luya: ACP Huiquilla, 2935 m a.s.l., CORBIDI 00038; Rodríguez de Mendoza: Vista Alegre: Hornillo, 3308 m a.s.l., CORBIDI 11747, 11752, 11763, 11767, 11770, 11773–74, 11788–89, 11792–94; Bongara: San Carlos: Corobamba, 3030–3050 m a.s.l., CORBIDI 21945, 21956, 21958. **San Martín**: Mariscal Cáceres: Camino Leimebamba-Los Chilchos, 3240 m a.s.l., CORBIDI 00592; San Martín: Tragadero-Las Piñas, 3235 m a.s.l., CORBIDI 10933.

Gastrotheca monticola — PERU: **Amazonas**: Bongara: Valera: Cocachimba, 1620 m a.s.l., CORBIDI 492; Quebrada El Atajo, 2416 m a.s.l., CORBIDI 19931; Opelel, 2655 m a.s.l., CORBIDI 19946–47; Leimebamba: Centro Poblado dos de Mayo, 2370 m a.s.l., CORBIDI

15890–91; Luya: Tingo: Ruinas de Silic, 1804 m a.s.l., CORBIDI 18602, 18605; Ruinas imperio – Bajo Kuelap, 2869 m a.s.l., CORBIDI 18616. **Piura**: Huancabamba: Sondor: Agupampa, 2625 m a.s.l., CORBIDI 14865–66. **Cajamarca**: Jaén: Pomahuaca, 2772 m a.s.l., CORBIDI 14887.

Gastrotheca sp. — PERU: **Amazonas**: Rodríguez de Mendoza: Vista Alegre, 3308 m a.s.l., CORBIDI 11776, 11768, 11775, 11777–78.

Gastrotheca oresbios — PERU: **Amazonas**: Chachapoyas: Abra Barro Negro, 3290 m a.s.l., CORBIDI 11076 (Holotype); **San Martín**: Mariscal Caceres: Quintecocha, 3119 m a.s.l., CORBIDI 11040.

Gastrotheca spectabilis — PERU: **Amazonas**: Rodríguez de Mendoza: Vista Alegre: Hornillo, 3308 m a.s.l., CORBIDI 11790 (Holotype), CORBIDI 11644, 11753, 11780–81, KU 342532.

Appendix 2

GenBank accession numbers for sequences used in this study.

Species	12S	16S	ND1	POMC	RAG1 (1)
Gastrotheca aguaruna KU 212026	—	KF723438	KF723462	KF723484	KF723505
Gastrotheca albolineata MNRJ 54401	KR559919	KR270407 + KR270425	KC844949	KR270365	KR138423
Gastrotheca antoniiochoai MUSM 27944	—	JN157622	KC844950	KC844972	KC844993
Gastrotheca aratia KU 212056	—	KF723443	KF723467	KF723489	KF723510
Gastrotheca argenteovirens KU 181168	DQ679233	DQ679383	DQ679342	DQ679311	—
Gastrotheca atympana MHNSM 18692	DQ679234	DQ679384	DQ679343	DQ679312	DQ679276
Gastrotheca aureomaculata KU 181194	DQ679235	DQ679385	DQ679344	—	DQ679277
Gastrotheca christiani FML 2881	DQ679236	DQ679386	DQ679345	DQ679313	DQ679278
Gastrotheca chrysosticta LM 58	DQ679237	DQ679387	DQ679346	—	DQ679279
Gastrotheca cornuta USNM 572472 + AMNH 107251	AY843591	AY843591	DQ679347	DQ679314	DQ679280
Gastrotheca cuencana QCAZ 42831	MG948913	MG948924	MH223474	MH223466	—
Gastrotheca dendronastes KU 181203	DQ679239	DQ679389	DQ679348	DQ679315	DQ679281
Gastrotheca dissimilis KU 181740	DQ679253	DQ679402	DQ679361	—	—
Gastrotheca dunni ICN 10059 + MHUA A 4800	DQ679240	KR270426	DQ679349	DQ679316	DQ679282
Gastrotheca ernestoi MNRJ 57129 + MNRJ 64000	KR559920	KR270408 + KR270427	KC844952	KR270366	KR138424
Gastrotheca espeletia KU203440		KJ489465	KJ489514	KJ489555	
Gastrotheca excubitor MUSM 26280	—	JN157623	—	—	—
Gastrotheca fissipes ZUFRJ 7901	—	—	JX262925	—	—
Gastrotheca fulvorufa CTMZ 07467	—	KC844929	KC844954	KC844977	KC844997
Gastrotheca galeata KU 181700	DQ679242	DQ679392	DQ679351	DQ679318	DQ679284
Gastrotheca gracilis DCC 006	DQ679243	—	—	DQ679319	—
Gastrotheca griswoldi MHNSM 20588	AM039716	AM039648	—	—	—
Gastrotheca guentheri KU 173112	DQ679245	DQ679393	DQ679353	DQ679321	DQ679285
Gastrotheca helenae KU 181070	DQ679246	DQ679394	DQ679354	DQ679322	DQ679286
Gastrotheca pseustes 1 QCAZ 45113	—	KC844923	KC844948	KC844970	—
Gastrotheca pseustes 2 QCAZ 42862 + TNHC 62492	AY326051	JX564866	KC844962	KC844986	KX208740
Gastrotheca litonedis KU 202690	DQ679247	DQ679395	DQ679355	DQ679323	DQ679287
Gastrotheca lojana QCAZ 42725 + KU 203546	—	KC844938	KC844964	KC844988	KJ489595
Gastrotheca longipes USNM 258905	DQ679248	DQ679396	DQ679356	DQ679324	DQ679288

Species	12S	16S	ND1	POMC	RAG1 (1)
Gastrotheca marsupiata KU 214813 + KU 214814	AY819356	DQ679397	AY819487	AY819105	DQ679289
Gastrotheca megacephala JLG 90 + CFBH T377	AY843592	AY843592	KC844953	KC844976	AY844381 + KC844996
Gastrotheca microdiscus CFBH T 1250 + CFBH T 3068	—	KC844932	KC844958	KC844979	KC844999
Gastrotheca monticola KU 212036	AY819357	DQ679398	AY819488	AY819106	DQ679290
Gastrotheca nebulanastes MUSM 27943 + MCZ 265218	—	JN157625	KC844959	KC844982	KC845001
Gastrotheca nicefori KU 181071	DQ679249	DQ679399	DQ679357	DQ679325	DQ679291
Gastrotheca ochoai KU173499	DQ679250	DQ679400	DQ679358	DQ679326	DQ679292
Gastrotheca oresbios CORBIDI 11076	—	KJ489461	KJ489509	KJ489552	KJ489588
Gastrotheca orophylax KU 178568	DQ679251	DQ679401	DQ679359	DQ679327	DQ679293
Gastrotheca ovifera KU 185758	DQ679252		—	DQ679360	—	—
Gastrotheca pachachacae MUSM 28492	—	JN157620	—	KC844983	KC845002
Gastrotheca peruana KU 207815		KF723451	KF723475	KF723497	—
Gastrotheca phalarosa CORBIDI 11044	—	KJ489459	KJ489507	KJ489551	KJ489585
Gastrotheca phelloderma MUSM 33350	—	MH756004	—	—	—
Gastrotheca plumbea KU 178499	DQ679254	DQ679403	DQ679362	DQ679328	DQ679294
Gastrotheca prasina MZUSP 147060 + MZUSP 17460	JX262891	KJ489476	JX262922	—	KJ489602
Gastrotheca psychrophila KU 142634	DQ679255	DQ679404	DQ679363	DQ679329	DQ679295
Gastrotheca rebeccae CORBIDI 08006	—	KC844937	KC844963	KC844987	—
Gastrotheca recava MZUSP 147044 + MZUSP 147042	JX262890	KJ489497	JX262921	—	KJ489604
Gastrotheca riobambae KU 178468 + KU 203516	DQ679256	DQ679405	DQ679364	KJ489580	DQ679296
Gastrotheca ruizi KU 200002	DQ679257	DQ679406	DQ679365	—	DQ679297
Gastrotheca yacuri QCAZ 21105	—	KC844939	KC844965	KC844989	—
Gastrotheca turnerorum QCAZ 47299	—	KC844934	KC844960	KC844984	—
Gastrotheca elicioi QCAZ 21213	—	KC844922	KC844947	—	—
Gastrotheca spectabilis CORBIDI 11790	—	KJ489464	KJ489513	KJ489554	KJ489592
Gastrotheca stictopleura MTD 45230	DQ679258	DQ679407	DQ679366	DQ679330	DQ679298
Gastrotheca testudinea QCAZ 16444	—	KC844940	KC844966	—	—
Gastrotheca trachyceps KU 181189	DQ679259	DQ679408	DQ679367	DQ679331	DQ679299
Gastrotheca walkeri Vz 8996	DQ679260	DQ679409	DQ679368	DQ679332	DQ679300
Gastrotheca weinlandii KU 143105	DQ679261	DQ679410	DQ679369	DQ679333	DQ679301
Gastrotheca zeugocystis MHNSM 18675	DQ679262	DQ679411	—	DQ679334	DQ679302
Gastrotheca sp. 1 IDLR 4073 (MNCN/ADN 566)	—	KR270428	—	—	—
Gastrotheca sp. 2 MNK 5286 + CBG 1020	AY843590	AY843590	KC844955	—	AY844380
Gastrotheca sp. 3 ZFMK 66954	—	KR270429	—	—	—
Gastrotheca sp. J CORBIDI 862	—	KJ489463	KJ489511	—	KJ489590
Gastrotheca sp. CORBIDI 11776	—	KJ489475	KJ489525	KJ489563	—
Gastrotheca sp. KU 173171	DQ679241	DQ679391	DQ679350	DQ679317	DQ679283
Gastrotheca gemma CORBIDI 21238	—	MW403923	—	—	—
Hemiphractus proboscideus	AY819358	DQ679413	AY819489	AY819107	DQ679304